

Design and Network Topology-Specific Renewal-Theoretic Analysis of a MAC Protocol for Asymmetric Full-Duplex WLANs

Rama Kiran¹, Neelesh B. Mehta², *Fellow, IEEE*, and Jestin Thomas

Abstract—The asymmetric network model, in which the access point (AP) is full-duplex (FD) capable while the other nodes are only half-duplex (HD) capable, is motivated by early-stage deployments of FD-capable networks. We propose a medium access control (MAC) protocol called asymmetric FD MAC (AFD-MAC) for this model. It leverages features such as random back-off and carrier sensing of the widely-used 802.11 HD MAC protocol, and it introduces two signals to exploit the FD capability of the AP. We also develop a general, network topology-specific renewal-theoretic analysis that characterizes the saturation throughput of AFD-MAC. It captures the differences in the statistical properties of the nodes and the AP due to differences in their duplexing capabilities or the number of hidden nodes. AFD-MAC can increase the throughput by a factor as large as two and can reduce head-of-line delay by a factor more than half compared to the conventional 802.11 HD MAC protocol. The gains depend on the ratio of the uplink to downlink packet lengths, network topology, and the extent of self-interference cancellation. A contrarian insight that emerges is that hidden nodes can enable the network to exploit its asymmetric FD capability.

Index Terms—Full-duplex communications, IEEE 802.11 standard, MAC protocol, renewal theory, WLAN.

I. INTRODUCTION

RECENT advances in wireless transceiver design techniques have made in-band full-duplex (FD), in which signal transmission and reception happen simultaneously and on the same frequency band, a practical reality [1]. It promises to double the data rate compared to conventional half-duplex (HD) communication without requiring more bandwidth. One critical challenge in implementing FD is

Manuscript received December 27, 2018; revised May 23, 2019 and September 7, 2019; accepted September 23, 2019. Date of publication October 1, 2019; date of current version December 17, 2019. This work was supported in part by the Visvesvaraya Ph.D. Scheme for Electronics and IT, and in part by the Indigenous 5G Test Bed Project funded by the Department of Telecommunications, India. The associate editor coordinating the review of this article and approving it for publication was V. Wong. (*Corresponding author: Rama Kiran.*)

R. Kiran and N. B. Mehta are with the Department of Electrical Communication Engineering, Indian Institute of Science (IISc), Bengaluru 560012, India (e-mail: ramakiranab@gmail.com; nbmehta@iisc.ac.in).

J. Thomas is with Maxilinear Inc., Bengaluru 560103, India (e-mail: jestin.307@gmail.com).

Color versions of one or more of the figures in this article are available online at <http://ieeexplore.ieee.org>.

Digital Object Identifier 10.1109/TCOMM.2019.2944907

self-interference, which is the interference caused by the transmitted signal to the receiver of the same node. A combination of wireless propagation, analog circuit, and digital-domain techniques have been developed in [2]–[4] to cancel it.

However, even with sufficient self-interference cancellation (SIC), several new protocol related challenges remain to be addressed to fully exploit FD in a wireless local area network (WLAN). Firstly, a new cross-interference arises between the nodes that transmit and receive unless they are hidden from each other. Secondly, the widely-used 802.11 HD medium access control (MAC) protocol, which employs carrier sensing multiple access (CSMA) and collision avoidance (CA), discourages simultaneous transmissions by multiple nodes. However, in FD, transmissions by multiple nodes are desirable and need to be facilitated by the MAC protocol.

A. Related Literature on MAC Protocols for FD

In the FD literature, MAC protocols have been designed for the following three system models: (i) Bi-directional model, in which all nodes in the system are FD and, therefore, any two nodes transmit and receive from each other simultaneously; (ii) Asymmetric model, in which only the access point (AP) is FD while all other nodes are HD; and (iii) Combined model, in which a mixture of FD and HD nodes exists in the system. In the following, we summarize the most pertinent literature. We shall refer to transmissions from the nodes to the AP as *uplink* transmissions and those from the AP to the nodes as *downlink* transmissions.

1) *Bi-Directional Model*: In the protocols proposed in [3], [5], [6], a node that wins the channel contention process transmits to the AP, which, in turn, transmits back to the same node. In [7], a node that wins the channel contention process establishes a bi-directional link with its destination node if the latter has data to transmit back. Else, either of these nodes establishes a simultaneous link with another node whose signal-to-interference ratio exceeds a minimum value. In [8], the nodes use their FD capability to simultaneously sense and transmit over orthogonal subcarriers. In [9], the nodes participate in the channel contention process only if the ratio of the data to be transmitted and received from the AP exceeds a threshold. The protocols in [10], [11] instead utilize a node's

FD capability to detect packet collisions in the channel and stop ongoing transmissions.

2) *Asymmetric Model*: In the power controlled MAC (PoCMAC) protocol [12], a node initially transmits a request-to-send (RTS) packet to the AP. Upon detecting this, the AP sends back a clear-to-send (CTS)-uplink packet to the node. Other nodes in the network overhear these packets and enter into a contention resolution phase, the winner of which receives from the AP. A similar two-stage channel contention-based protocol is proposed in [13]. In the MASTaR protocol [14], it is assumed that the AP knows the signal-to-interference-plus-noise ratio (SINR) at all the nodes in the network. While receiving from a node, the AP transmits to another node that maximizes the ratio of the received signal strength to a minimum desired signal strength at the nodes. Instead, in [15], the AP transmits to the node that maximizes a throughput-related performance measure.

The A-duplex protocol in [16] uses a preamble transmission to ensure uplink and downlink packet alignment and to capture the downlink packet. Furthermore, it collects information about the SINRs at the nodes to determine which node to transmit to. In [17], a node initiates a transmission and the AP decides whether to communicate using HD or FD, its destination node, and transmit power. In [18], the AP starts transmitting a packet to a node. Meanwhile, the other nodes in the network contend using the back-off timer scheme to transmit simultaneously on the uplink.

3) *Combined Model*: In the Contraflow protocol [19], a node that wins the channel contention process starts transmitting to its destination node. The destination node, in turn, selects another node depending on its past successful transmissions and transmits to it simultaneously. In the Janus protocol [20], the AP schedules nodes taking into account their data packet queue lengths and the feedback about inter-node interference received from all the nodes. In [21], back-off timer values are exchanged between nodes to time-synchronize the AP and node transmissions to create FD opportunities. In [22], the FD capability of the secondary users is used to sense the activity of the primary users in a cognitive radio environment. In [23], multiple nodes make time-separated smaller uplink transmissions while the AP transmits for a longer duration.

B. Contributions

In this paper, we propose and analyze a new asymmetric FD MAC (AFD-MAC) protocol for the asymmetric model that exploits the FD capability of the AP. This model is well motivated because FD is likely to be commercially implemented first in more advanced transceivers, such as the AP, given the specialized hardware and algorithms required to enable it. We make the following contributions.

1) *AFD-MAC Protocol*: It leverages distributed features of the widely-used 802.11 MAC protocol such as random back-off, carrier sensing, and RTS-CTS exchange. To leverage the AP's FD capability, it introduces two signals, namely, an FD-RTS packet, which is transmitted by the AP to a node to inform it that it can transmit a data packet to the AP, and an FD-busy tone (FBT),

which the AP broadcasts to all the nodes to prevent the hidden nodes from transmitting and colliding.

- 2) *Renewal-Theoretic Fixed-Point Analysis*: We present a decoupling approximation based [24] accurate renewal-theoretic analysis for the saturation throughput of AFD-MAC in networks with hidden nodes. We do so for the collision model. The saturation throughput is a widely-studied performance measure, which often characterizes the maximum system throughput in heavy data traffic conditions [25]. The power of this approach can be seen from its ability to accurately characterize the general scenario in which different nodes see different sets of hidden nodes, which can be of different cardinalities. It leads to different statistical parameters for the AP and each of the nodes.
- 3) *Performance Benchmarking*: We present extensive simulation results that benchmark the saturation throughput and head-of-line (HoL) delay of the AP and the nodes for specific network topologies and when averaged over many topologies. The HoL delay, which has been less investigated in the FD literature, is the average service time of a packet at the HoL position of the data packet queue in a node [26]. It is a performance measure of relevance to higher layers in the protocol stack. An important and a rather contrarian insight these results bring out is the constructive role that hidden nodes play in enabling asymmetric FD, despite the increased likelihood of collisions that they beget. We observe that AFD-MAC can increase the saturation throughput compared to the 802.11 HD MAC by a factor of up to two and reduce the HoL delay by more than half. The performance gains depend on the network topology, the asymmetry in the uplink and downlink packet transmission durations, and the extent of SIC.

Comments and Comparisons: While there are similarities between AFD-MAC and the protocols proposed in the literature, there are also several differences. The protocols in [12], [15] do not consider the case where the AP contends for channel access. In [14], [16], the AP does not exploit its FD capability when it initiates a transmission. The two-stage channel contention processes that are employed in [12], [13] to select the nodes for uplink and downlink transmissions require additional control signaling and time. In [10], [11], [22], the FD capability is used to detect packet collisions in the channel, but not for simultaneous uplink and downlink transmissions. In [21], an FD transmission can occur between the AP and a node only if their back-off timers are synchronized. AFD-MAC instead uses a single-stage contention process. It allows the AP to initiate a transmission and better exploits its FD capability. We note that the busy tone has been used in several works, e.g., [3], [13], [16], [27]. However, one subtle difference is that in AFD-MAC, the AP can broadcast the FBT in two instances – at the time of receiving an RTS packet and when the downlink transmission completes before the uplink transmission.

Only simulation results are presented for the asymmetric models studied in [12], [14], [15]. The Markov chain-based analyses for the asymmetric model in [16] and for the other

models in [5], [27] assume that the channel access statistics of all the nodes are the same even in the presence of hidden nodes. The simultaneous uplink and downlink transmissions that can occur, the possibility of a node serving as a secondary transmitter in the AP-initiated scenario, and our above general model for hidden nodes make our approach different even from the renewal-theoretic analysis for the conventional HD MAC protocols in [24] and the references therein.

To the best of our knowledge, a combination of an effective MAC protocol for the asymmetric model coupled with a general renewal-theoretic analysis, which provides node-specific and network topology-specific expressions for the saturation throughput, has not been presented before for an FD-MAC protocol. In addition, we study the head-of-line (HoL) delay and the effect of an increase in the packet error rate due to imperfect SIC. Furthermore, our topology-averaged results are new and insightful.

C. Outline and Notation

The outline of the paper is as follows. We present the system model and describe AFD-MAC in Section II. We analyze AFD-MAC in Section III. Simulation results and performance benchmarking are presented in Section IV, and our conclusions follow in Section V.

Notation: The expectation with respect to a random variable (RV) X is denoted by $\mathbb{E}_X[\cdot]$, with the subscript dropped when it is obvious from context. $\mathbb{1}_{\{a\}}$ denotes the indicator function; it is 1 if a is true and is 0 otherwise. For a set \mathcal{A} , its complement is denoted by \mathcal{A}^c , and its cardinality by $|\mathcal{A}|$. For a null set \mathcal{A} , the summation $\sum_{i \in \mathcal{A}}(\cdot)$ is 0. The probability of an event A is denoted by $P(A)$, and the conditional probability of A given B is denoted by $P(A|B)$.

II. SYSTEM MODEL AND PROTOCOL DESCRIPTION

Consider an asymmetric network in which N nodes communicate with an AP that operates in the infrastructure mode. The AP is indexed by 0 and the node indices belong to the set $\mathbb{N} = \{1, 2, \dots, N\}$. Time is slotted with a slot duration δ . In our analysis, we assume that all transmissions start and end at slot boundaries [25], [28]. This does not affect the practical operation of the protocol because transmissions are specified as commencing a time delay after a previous transmission ends, as is done in the conventional 802.11 MAC protocol [25], [28]. The *neighbor list* \mathcal{N}_i of node i denotes the set of nodes (excluding the AP) that are in its interference range. A node can construct its neighbor list by listening to past data packet transmissions from its neighbors. By default, $i \in \mathcal{N}_i$. Therefore, \mathcal{N}_i^c constitutes the set of hidden nodes of node i . This model is illustrated in Fig. 1.

We assume that the AP knows the neighbor lists of the N nodes. This can be achieved by making a node occasionally send its neighbor list to the AP. It can be done using, for example, management frames of the 802.11 MAC protocol or by piggybacking it with its data packets. In low mobility environments, where WLANs are often used, the overhead of occasionally updating the neighbor list is amortized over time and has a negligible impact on the throughput. This is similar to the channel state feedback models assumed in [14], [16], [20].

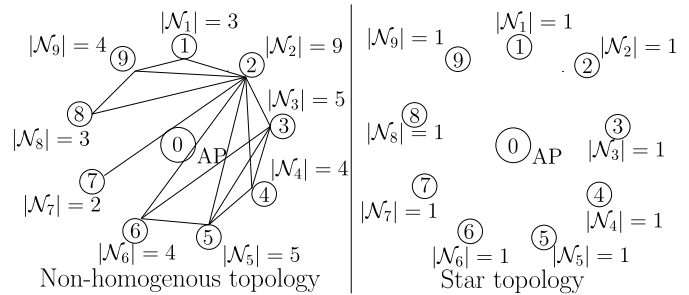


Fig. 1. Illustration of two different network topologies with an FD-capable AP and $N = 9$ HD nodes. The absence of a line between two nodes indicates that they are hidden from each other.

A. AFD-MAC Protocol

In our description of AFD-MAC below, we first specify the protocol for the scenario in which the residual self-interference is negligible. Thereafter, in Section II-B, we model imperfect SIC, its impact, and the modifications to the protocol to handle packet errors caused by it.

AFD-MAC adopts the RTS-CTS-based channel contention mechanism of 802.11 HD MAC in order to deal with hidden nodes [25], [28]. When the back-off timer of a node or the AP becomes zero, it starts transmitting an RTS packet of duration T_{RTS} to its destination. We shall refer to it as the *primary transmitter*. The destination sends back a CTS packet of duration T_{CTS} after a short inter-frame space (SIFS) of duration T_{SIFS} . Thereafter, the primary transmitter starts transmitting its data packet after another T_{SIFS} seconds.

The following three scenarios arise depending on who initiated the RTS packet transmission:

1. *Node-Initiated Scenario:* When a node, say A , initiates an RTS packet transmission, the AP starts broadcasting an FBT, which is a sinusoidal signal, immediately after it senses the transmission and until it receives the entire RTS packet. This ensures that the nodes hidden from the primary transmitter (node A) freeze their back-off timers and do not collide with its RTS packet. This is an improvement over the conventional 802.11 HD MAC in which the hidden nodes freeze their timers only after hearing the CTS from the AP. Thereafter, the AP simultaneously transmits a data packet to a destination node, say B , that is hidden from node A . We shall refer to the AP as the *secondary transmitter* here. However, if there is no hidden node, then only node A transmits a data packet. This scenario is illustrated in Fig. 2(a).

2. *AP-Initiated Scenario:* Here, the AP is the primary transmitter. After transmitting its RTS packet to a destination node, say A , it transmits an FD-RTS¹ packet to another node, say B , when the destination node is transmitting its CTS packet back to the AP. This informs node B that it can transmit a data packet in parallel T_{SIFS} seconds after the FD-RTS transmission ends. The selection of node B is at the discretion of the AP. For example, it can select a node based

¹FD-RTS can be implemented by making minor changes to the existing RTS frame in the 802.11 MAC protocol. For example, bits b_4 to b_7 in the frame control field can be changed from 1011 in the *RTS frame* to 1000 to indicate FD-RTS.

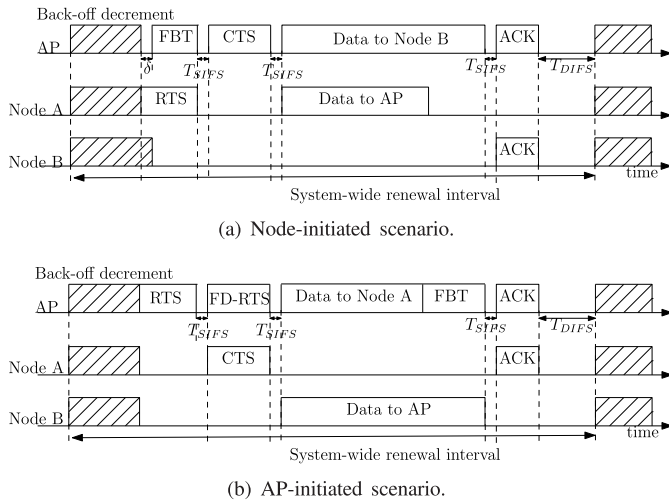


Fig. 2. Illustrations of the time traces of AFD-MAC in the node-initiated and AP-initiated scenarios. Here, nodes A and B are hidden from each other.

on the information about the queue lengths at the nodes that is available to it. We shall refer to node *B* as the *secondary transmitter* here. However, if node *A* has no hidden node, then only the AP transmits a data packet. This scenario is illustrated in Fig. 2(b).

3. *AP-cum-Node-Initiated Scenario*: When the back-off timers of the AP and one of the nodes, say *A*, expire in the same slot, then both AP and node *A* are primary transmitters that transmit their RTS packets simultaneously. Let node *B* be the destination node of the AP. If nodes *A* and *B* are hidden from each other, then both RTS packets are decoded successfully. After T_{SIFS} seconds, the AP and node *B* transmit CTS packets to node *A* and the AP, respectively. Thereafter, upon successfully receiving these CTS packets, both AP and node *A* start transmitting their data packets after T_{SIFS} seconds. Else, if nodes *A* and *B* are not hidden from each other, then the RTS packet of the AP will not be decoded by node *B* since it will collide with that of node *A*.

1) *Asymmetric Data Packet Transmission Durations*: In the above scenarios, when the AP and a node, say *A*, transmit data packets and if the AP finishes its transmission before node *A*, then it broadcasts the FBT until the node finishes its transmission. Consequently, the hidden nodes of node *A* do not start decrementing their back-off timers and eventually collide with its ongoing transmission. This is also illustrated in Fig. 2(b).

Once both primary and secondary transmitters have finished their transmissions, the AP and its destination node send back acknowledgments (ACK) of duration T_{ACK} after T_{SIFS} seconds.

2) *RTS Packet Collisions and Their Effect*: In case two or more RTS packets collide at a receiver, then none of them can be decoded by it [25], [28]. In such a scenario, the receiver does not back send a CTS packet. RTS packet decoding errors are also treated as the collisions by the transmitters, as is the case in the 802.11 HD MAC. The node or the AP, whose RTS packet has collided, chooses a new back-off timer value with uniform probability from a contention window. After a distributed coordinate function inter-frame

space (DIFS) of duration T_{DIFS} , it starts decrementing it to attempt a retransmission. The contention window size is doubled after every collision subject to a maximum of CW_{max} . The initial contention window size is CW_{min} . The data packet is dropped after L unsuccessful RTS packet retransmission attempts.

The effect of the RTS packet collisions is different in the above three scenarios. In the node-initiated scenario, RTS packets collide at the AP when two or more nodes initiate their transmissions in the same slot. This also happens when nodes hidden from each other start transmitting their RTS packets in two consecutive slots, since they cannot sense each other's transmissions. The channel then remains idle for a duration of T_{DIFS} and the colliding nodes set new back-off timer values. In the AP-initiated scenario, no RTS packet collision can occur since only the AP transmits initially and determines the secondary transmitter.

In the AP-cum-node-initiated scenario, let the AP and node *i* transmit RTS packets simultaneously to node *j* and the AP, respectively. RTS packets collide at the AP when at least one other node starts transmitting an RTS packet simultaneously along with node *i*. RTS packets collide at node *j* if at least one other node in \mathcal{N}_j starts transmitting an RTS packet simultaneously. In this scenario, multiple outcomes are possible. If the RTS packet collision occurs only at the AP, then the AP can still transmit a data packet to node *j*. Else, if the collision occurs only at node *j*, then the AP still receives a data packet from node *i*. At this time, the AP knows that its RTS packet has collided and it can instead transmit a data packet to a node in \mathcal{N}_i^c . No data packet transmission occurs if the RTS packets sent by the AP and node *i* both collide.

3) *Compatibility with 802.11 HD MAC and Protocol Changes*: AFD-MAC is compatible with HD nodes that operate using the conventional 802.11 MAC protocol and are unaware of AFD-MAC. These nodes can transmit to the AP or receive from it as before. This is possible because AFD-MAC reuses CSMA/CA with RTS-CTS to determine who gets to transmit. However, the nodes cannot transmit to the AP as secondary transmitters or receive from it when it is a secondary transmitter because of the differences in the protocols. There are minor changes in the protocol when a node or the AP is the secondary transmitter. Here, a node, when chosen by the AP, can transmit or receive data packets without the RTS-CTS exchange. Another change is that the HD nodes feed back their neighbor lists to the AP, albeit occasionally. Changes are needed at the AP in order to exploit its FD capability. These include two new signals, namely, FBT and FD-RTS.

B. With Imperfect SIC

We now model imperfect SIC and its impact. Imperfect SIC leads to residual self-interference at the AP. When the AP transmits in FD, the SINR at the AP is given by

$$\zeta = \frac{P_{RX}}{kTBF + \frac{P_{TX}}{\Delta}}, \quad (1)$$

where P_{RX} is the received power, P_{TX} is the transmit power of the AP, $\Delta \geq 1$ is the SIC factor, k is the Boltzman's constant,

T is the temperature, F is the noise figure, and B is the bandwidth. Here, P_{TX}/Δ is the residual self-interference at the AP. In HD, ζ is equal to $P_{\text{RX}}/(kTBF)$, which is greater than the SINR in (1). The reduction in SINR translates to a higher data packet error rate (PER) in FD. However, the PER of an RTS/CTS packet remains negligible when it is shorter and is encoded using a low rate modulation and coding scheme. This is because the minimum SINR at which the RTS packets can be decoded is several dBs lower than that of the data packets [29].

We modify the AFD-MAC protocol to handle decoding errors due to imperfect SIC as follows. If a data packet is received in error at the AP, it transmits a negative-acknowledgment (NACK) instead of an ACK.² Since the packet error did not occur due to a collision, the node contends for the channel again with the same contention window size. However, the packet gets dropped after L unsuccessful retransmissions or RTS transmissions.

III. RENEWAL-THEORETIC FIXED-POINT ANALYSIS

We now analyze the saturation throughput of AFD-MAC for any given network topology for the collision model. We shall assume that the residual self-interference at the AP is zero and the probability of decoding error due to noise is negligible [16], [30]. We note that the HoL delay and non-zero PERs due to imperfect SIC can also be analyzed in a similar manner. However, we do not present this analysis due to space constraints. Subsequently, in Section IV-C, we numerically study the impact of imperfect SIC on the saturation throughput.

We use the following two conventions: 1) In the AP-initiated scenario, the AP selects its destination node with equal probability from the set \mathbb{N} , and the secondary transmitter with equal probability from among the nodes hidden from its destination node; and 2) In the node-initiated scenario, the AP selects its destination node with equal probability from the hidden nodes of the primary transmitter. Note that any node that is selected by the AP will have a packet to transmit with probability one in the saturation throughput analysis.

To develop a tractable analysis for AFD-MAC, we employ the following two classical *decoupling approximations* [28]:

- 1) Conditioned on a node $i \in \mathbb{N}$ transmitting an RTS packet, the event that this packet collides is independent of its previous transmissions. Let the probability of this event be denoted by γ_i , which we shall refer to as the *conditional collision probability*. Similarly, for the AP, let Γ_i denote the conditional collision probability when it transmits an RTS packet to node i .
- 2) The N nodes and the AP attempt RTS packet transmissions independent of the states of all other nodes. In a slot, a node i or the AP transmits an RTS packet with probability β_i , for $i \in \mathbb{N} \cup \{0\}$, which we shall refer to as the *attempt rate*.

An important feature of our model is that the attempt rate and conditional collision probabilities are node-specific.

²NACK can be implemented by reusing the frame structure of 802.11's ACK and making minor modifications to it. For example, bits $b4$ to $b7$ in the frame control field can be changed from 1101 in the ACK frame to 1001.

This accounts for the fact that the number of hidden nodes can be different for different nodes, which affects the protocol's behavior. For the same reason, the conditional collision probabilities of the AP are also dependent on its destination nodes.

A. Attempt Rate and Conditional Collision Probability

We analyze a node-specific renewal process to derive expressions for the attempt rates of the AP and the N nodes in terms of the conditional collision probabilities. Let $R_i^{(j)}$ and $\chi_i^{(j)}$ denote the number of RTS packet transmission attempts made and the total back-off time needed, respectively, by a node i to successfully transmit its j^{th} data packet. From the decoupling approximations, the back-off process of node i forms a node-specific renewal process with renewal intervals $\chi_i^{(j)}$, for $j \geq 1$, and with the renewal instants being the start of back-off timer decrements for the first RTS packet transmission attempts. From the renewal reward theorem [31, Chap. 5.4], the attempt rate β_i is given by

$$\beta_i = \frac{\mathbb{E} \left[R_i^{(j)} \right]}{\mathbb{E} \left[\chi_i^{(j)} \right]}, \quad \text{for } i \in \mathbb{N} \cup \{0\}. \quad (2)$$

Let w_0 be the initial back-off timer value of the node/AP; it is chosen with equal probability from the set $\{0, 1, \dots, \text{CW}_{\min} - 1\}$. And, let w_m be the timer value after the m^{th} collision; it is chosen with equal probability from the set $\{0, 1, \dots, \text{CW}_m - 1\}$. Here, CW_m is the contention window size after the m^{th} collision. During the contention phase, let s_i denote the probability of node $i \in \mathbb{N}$ receiving a request from the AP to transmit a packet as a secondary transmitter in a slot. Similarly, let s'_i denote the probability of the AP becoming a secondary transmitter and transmitting a packet to node i . The following two results relate the attempt rates with the conditional collision probabilities of the AP and the N nodes.

Claim 1: For a node $i \in \mathbb{N}$, the attempt rate is given by

$$\beta_i = \frac{1}{\sum_{k=0}^L \bar{T}_k(s_i, \gamma_i) + \bar{T}_{\text{drp}}(s_i, \gamma_i)} \left(\sum_{k=1}^{L+1} k \gamma_i^{k-1} \times \left[\prod_{m=0}^{k-1} z_m(s_i) \right] - \sum_{k=1}^L k \gamma_i^k \left[\prod_{m=0}^k z_m(s_i) \right] \right), \quad (3)$$

where

$$s_i = \frac{\beta_0}{N} \left[\prod_{k=1}^N (1 - \beta_k) \right] \sum_{l \in \mathcal{N}_i^c} \frac{1}{|\mathcal{N}_l^c|}, \quad (4)$$

$$\begin{aligned} z_m(s_i) &= \mathbb{E}_{w_m} \left[(1 - s_i)^{w_m+1} \right], \\ &= \frac{(1 - s_i) \left(1 - (1 - s_i)^{\text{CW}_m} \right)}{s_i \text{CW}_m}. \end{aligned} \quad (5)$$

Here, $\bar{T}_k(s_i, \gamma_i)$ is the contribution to $\mathbb{E}[\chi_i^{(j)}]$ from the renewal cycles in which k RTS collisions occur. It equals

$$\begin{aligned} \bar{T}_k(s_i, \gamma_i) &= \gamma_i^k \left[(1 - \gamma_i) \sum_{l=0}^k \frac{z'_l(s_i) z_k(s_i)}{z_l(s_i)} \right. \\ &\quad + (1 - z_k(s_i)) \sum_{l=0}^{k-1} \frac{z'_l(s_i)}{z_l(s_i)} \\ &\quad \left. + \frac{1 - z_k(s_i) - s_i z'_k(s_i)}{s_i} \right] \prod_{m=0}^{k-1} z_m(s_i), \quad (6) \end{aligned}$$

where $z'_m(s_i) = \mathbb{E}_{w_m} \left[(w_m + 1) (1 - s_i)^{w_m + 1} \right] = (1 - s_i) \left[1 - (1 + s_i \text{CW}_m) (1 - s_i)^{\text{CW}_m + 1} \right] / (s_i^2 \text{CW}_m)$.

And, $\bar{T}_{\text{drp}}(s_i, \gamma_i)$ is the contribution from the renewal cycles in which data packets are dropped:

$$\bar{T}_{\text{drp}}(s_i, \gamma_i) = \gamma_i^{L+1} \sum_{k=0}^L z'_k(s_i) \left[\prod_{m=0, m \neq k}^L z_m(s_i) \right]. \quad (7)$$

Proof: The proof is relegated to Appendix A. ■

Claim 2: For the AP, the attempt rate is given by

$$\begin{aligned} \beta_0 &= \frac{1}{\sum_{i=1}^N \left(\sum_{k=0}^L \bar{T}_k(s'_i, \Gamma_i) + \bar{T}_{\text{drp}}(s'_i, \Gamma_i) \right)} \\ &\quad \times \sum_{i=1}^N \left(\sum_{k=1}^{L+1} k \Gamma_i^{k-1} \left[\prod_{m=0}^{k-1} z_m(s'_i) \right] \right. \\ &\quad \left. - \sum_{k=1}^L k \Gamma_i^k \left[\prod_{m=0}^k z_m(s'_i) \right] \right), \quad (8) \end{aligned}$$

where

$$s'_i = (1 - \beta_0) \sum_{k \in \mathcal{N}_i^c} \frac{\beta_k \left[\prod_{l=1, l \neq k}^N (1 - \beta_l) \right] \left[\prod_{l \in \mathcal{N}_k^c} (1 - \beta_l)^2 \right]}{|\mathcal{N}_k^c|}. \quad (9)$$

Proof: The proof is relegated to Appendix B. ■

The next result relates the conditional collision probabilities with the attempt rates.

Claim 3: The conditional collision probability γ_i of a node $i \in \mathbb{N}$ is given by

$$\begin{aligned} \gamma_i &= 1 - (1 - \beta_0) \left[\prod_{j=1, j \neq i}^N (1 - \beta_j) \right] \left[\prod_{j \in \mathcal{N}_i^c} (1 - \beta_j)^2 \right] \\ &\quad - \beta_0 \prod_{j=1, j \neq i}^N (1 - \beta_j). \quad (10) \end{aligned}$$

The conditional collision probability Γ_i , for $i \in \mathbb{N}$, of the AP is given by

$$\Gamma_i = 1 - \prod_{j \in \mathcal{N}_i} (1 - \beta_j). \quad (11)$$

Proof: The proof is relegated to Appendix C. ■

1) Comments: We note that (3) and (8) are different compared to [25, (1)]. This is because a node that is participating in the contention process can withdraw from it if it becomes a secondary transmitter. Similarly, (10) is different from [25, (2)] because of the presence of hidden nodes.

2) Fixed-Point Equations: Equations (3), (8), (10), and (11) constitute $(3N + 1)$ -dimensional fixed-point equations in $(3N + 1)$ variables. Since these equations constitute a continuous mapping from $[0, 1]^{3N+1}$ to $[0, 1]^{3N+1}$, by Brouwer's fixed-point theorem, there exists a fixed-point in the range $[0, 1]^{3N+1}$. We solve for it numerically to obtain $\gamma_1, \dots, \gamma_N$, $\Gamma_1, \dots, \Gamma_N$, and β_0, \dots, β_N .³

B. Saturation Throughput Analysis

To derive an expression for the saturation throughput Ψ , we now consider the system-wide renewal process, which is the aggregate process of the packet transmission attempts of the AP and the N nodes. In it, the time instant at which the AP or the N nodes start transmitting RTS packets after the idle period is a renewal instant, and the time period between two such instants is the renewal interval. Let T be the duration of the renewal interval. From the renewal reward theorem, it follows that

$$\Psi = \frac{\sum_{i=0}^N \mathbb{E}[\theta_i]}{\mathbb{E}[T]}, \quad (12)$$

where θ_0 and θ_i , for $i \in \mathbb{N}$, are the number of bits transmitted by the AP and node i , respectively, in a renewal interval, and $\mathbb{E}[\theta_i] / \mathbb{E}[T]$ is the corresponding saturation throughput.

1) Evaluation of $\mathbb{E}[\theta_i]$: Let ϕ_0 and ϕ_i denote the average number of bits in the data packets transmitted by the AP and node i , respectively. This average can also account for adaptation of the rate to variations in the SINR due to fading.

Claim 4: For a node $i \in \mathbb{N}$, $\mathbb{E}[\theta_i]$ is given by

$$\begin{aligned} \mathbb{E}[\theta_i] &= \frac{\beta_i \phi_i \left[\prod_{j=1, j \neq i}^N (1 - \beta_j) \right]}{1 - \prod_{k=0}^N (1 - \beta_k)} \left(\beta_0 + (1 - \beta_0) \right. \\ &\quad \left. \times \prod_{j \in \mathcal{N}_i^c} (1 - \beta_j)^2 + \frac{\beta_0 (1 - \beta_i)}{N} \sum_{j \in \mathcal{N}_i^c} \frac{1}{|\mathcal{N}_j^c|} \right). \quad (13) \end{aligned}$$

For the AP, $\mathbb{E}[\theta_0]$ is given by

$$\begin{aligned} \mathbb{E}[\theta_0] &= \frac{\beta_0 \phi_0}{N \left[1 - \prod_{k=0}^N (1 - \beta_k) \right]} \sum_{i=1}^N \left(\prod_{j \in \mathcal{N}_i} (1 - \beta_j) \right. \\ &\quad \left. + \sum_{j \in \mathcal{N}_i} \beta_j \left[\prod_{k=1, k \neq j}^N (1 - \beta_k) \right] 1_{\{|\mathcal{N}_j^c| \neq 0\}} \right) \\ &\quad + \frac{(1 - \beta_0) \phi_0}{1 - \prod_{k=0}^N (1 - \beta_k)} \sum_{i=1}^N \beta_i \left[\prod_{j=1, j \neq i}^N (1 - \beta_j) \right] \\ &\quad \times \left[\prod_{j \in \mathcal{N}_i^c} (1 - \beta_j)^2 \right] 1_{\{|\mathcal{N}_i^c| \neq 0\}}. \quad (14) \end{aligned}$$

Proof: The proof is relegated to Appendix D. ■

Equation (13) brings out two different effects of hidden nodes. First, if the number of hidden nodes of node i is large, then $\prod_{j \in \mathcal{N}_i^c} (1 - \beta_j)^2$ is small. This reduces $\mathbb{E}[\theta_i]$. Instead, if there are no hidden nodes, then the third term in the summation vanishes, which again reduces $\mathbb{E}[\theta_i]$.

³It is not known if the fixed point is unique. In general, except for simple networks, proving uniqueness is hard or multiple fixed points can exist [24].

2) *Evaluation of $\mathbb{E}[T]$* : The average duration $\mathbb{E}[T]$ of a renewal interval is given as follows.

Claim 5: The average duration $\mathbb{E}[T]$ is given by

$$\mathbb{E}[T] = \bar{T}_{\text{idle}} + \bar{T}_s + \bar{T}_{\text{no-tx}}, \quad (15)$$

where $\bar{T}_{\text{idle}} = \left[1 - \prod_{k=0}^N (1 - \beta_k)\right]^{-1}$ is the expected idle period duration in a renewal interval. \bar{T}_s is the contribution from the renewal intervals in which successful data packet transmission(s) occur. It is given by

$$\begin{aligned} \bar{T}_s = & \frac{\beta_0 \prod_{i=1}^N (1 - \beta_i)}{1 - \prod_{k=0}^N (1 - \beta_k)} \sum_{i=1}^N \left(\frac{\Psi_1(i)}{N} + \frac{\beta_i \Psi_2(i)}{1 - \beta_i} \right) \\ & + \frac{1 - \beta_0}{1 - \prod_{k=0}^N (1 - \beta_k)} \sum_{i=1}^N \beta_i \left[\prod_{j=1, j \neq i}^N (1 - \beta_j) \right] \\ & \times \left[\prod_{j \in \mathcal{N}_i^c} (1 - \beta_j)^2 \right] \Psi_2(i), \quad (16) \end{aligned}$$

where $\Psi_1(i) = \max\{T_{\text{AP}}, T_{\text{node}} \mathbf{1}_{\{|\mathcal{N}_i^c| \neq 0\}}\}$, $\Psi_2(i) = \max\{T_{\text{AP}} \mathbf{1}_{\{|\mathcal{N}_i^c| \neq 0\}}, T_{\text{node}}\}$, $T_{\text{AP}} = \sigma_{\text{AP}} + T_{\text{DIFS}} + 3T_{\text{SIFS}} + T_{\text{RTS}} + T_{\text{CTS}} + T_{\text{ACK}}$, and $T_{\text{node}} = \sigma_{\text{node}} + T_{\text{DIFS}} + 3T_{\text{SIFS}} + T_{\text{RTS}} + T_{\text{CTS}} + T_{\text{ACK}}$. Here, σ_{AP} and σ_{node} denote the durations of the data packets transmitted by the AP and the N nodes, respectively. And, $\bar{T}_{\text{no-tx}}$ is the contribution from the renewal intervals in which no successful data packet transmission occurs. It is given by

$$\begin{aligned} \bar{T}_{\text{no-tx}} = & \frac{T_{\text{abrt}} \beta_0}{N \left[1 - \prod_{k=0}^N (1 - \beta_k)\right]} \sum_{i=1}^N \left(1 - \prod_{j \in \mathcal{N}_i} (1 - \beta_j) \right. \\ & \left. - \sum_{j \in \mathcal{N}_i^c} \beta_j \left[\prod_{k=1, k \neq j}^N (1 - \beta_k) \right] \right) \\ & + \frac{T_{\text{abrt}} (1 - \beta_0)}{1 - \prod_{k=0}^N (1 - \beta_k)} \left(1 - \prod_{i=1}^N (1 - \beta_i) \right. \\ & \left. - \sum_{i=1}^N \beta_i \left[\prod_{j=1, j \neq i}^N (1 - \beta_j) \right] \left[\prod_{j \in \mathcal{N}_i^c} (1 - \beta_j)^2 \right] \right), \quad (17) \end{aligned}$$

where $T_{\text{abrt}} = T_{\text{DIFS}} + T_{\text{RTS}}$.

Proof: The proof is relegated to Appendix E. ■

Explanation: In the above expressions, T_{AP} is the transmission duration when only the AP transmits and T_{node} is the corresponding duration when only a node transmits. These two need not be the same. The term $\Psi_1(i)$ in (16) is the transmission duration in the AP-initiated scenario when node i is the destination node of the AP. If the destination node has no hidden nodes, then only the AP transmits with duration T_{AP} , else both AP and a node transmit with duration $\max\{T_{\text{AP}}, T_{\text{node}}\}$. Therefore, $\Psi_1(i) = \max\{T_{\text{AP}}, T_{\text{node}} \mathbf{1}_{\{|\mathcal{N}_i^c| \neq 0\}}\}$. Similarly, $\Psi_2(i)$ is the transmission duration in the node-initiated scenario when node i initiates a transmission. Only the primary transmitter transmits if it has no hidden nodes, else both it and

the AP transmit. Hence, $\Psi_2(i) = \max\{T_{\text{AP}} \mathbf{1}_{\{|\mathcal{N}_i^c| \neq 0\}}, T_{\text{node}}\}$. These expressions capture the effect of asymmetric uplink and downlink data packet durations.

IV. NUMERICAL RESULTS

We now present Monte Carlo simulation results of AFD-MAC to evaluate its performance and assess the accuracy of the analysis. To gain insights, we present two sets of results. First, we study specific network topologies to compare and understand the behavior of each node. Second, we present results that are averaged over 1000 different network topologies. For each topology, we run the simulation for 10^6 slots. This is not computationally feasible with tools such as network simulator (ns). Consequently, a time-driven simulator written in the C programming language was developed. As in the analysis, we focus on the collision model. This enables us to assess the impact of the decoupling approximations on the accuracy of the analysis, and also enables us to generate a comprehensive set of topology-averaged results. A simulation campaign based on alternate physical layer abstractions such as the capture model [32, Chap. 8] is beyond the scope of this paper.

In the topology-averaged results, we benchmark the saturation throughput of the AFD-MAC protocol against the following: (1) Conventional 802.11 HD MAC with the RTS-CTS mechanism; (2) Protocol in which FD is allowed except in the AP-initiated scenario [12], [14]–[16]; (3) FD protocol with two-stage back-off to select primary and secondary transmitters [12], [13]; and (4) FD protocol with time-separated acknowledgments [12], [16]. In the above FD protocols, other aspects are kept the same as AFD-MAC to ensure a fair comparison. The simulation parameters, which are adopted from the 802.11a standard [33], are: $\delta = 9 \mu\text{s}$, $T_{\text{DIFS}} = 34 \mu\text{s}$, $T_{\text{SIFS}} = 16 \mu\text{s}$, $\text{CW}_{\text{min}} = 32$, $\text{CW}_{\text{max}} = 1024$, $L = 5$, $T_{\text{RTS}} = 52 \mu\text{s}$, and $T_{\text{CTS}} = T_{\text{ACK}} = 44 \mu\text{s}$. Data packets are transmitted at a rate $\Omega_d = 12 \text{ Mbps}$, control packets at a rate $\Omega_c = 6 \text{ Mbps}$, and $\phi_0 = \phi_i = 1,000$ bytes. Therefore, $\sigma_{\text{AP}} = \sigma_{\text{node}} = 692 \mu\text{s}$. We first show results with perfect SIC. Thereafter, in Section IV-C, we show results with imperfect SIC.

A. Results for a Given Network Topology

Fig. 3(a) plots the saturation throughput of each node normalized with respect to the rate Ω_d for the non-homogeneous topology shown in Fig. 1, the star topology (in which $|\mathcal{N}_i| = 1$, for $i \in \mathbb{N}$), and the fully connected topology (in which $|\mathcal{N}_i| = N$, for $i \in \mathbb{N}$). We observe that the downlink throughput of the AP (node 0) exceeds the uplink throughput of the N nodes in both topologies. Also, the throughput of the AP depends on the network topology; it is more in the network with more hidden nodes. In the non-homogeneous topology, node 2, which has no hidden nodes, has the highest saturation throughput among the N nodes. In the fully connected topology, no hidden nodes exist. Hence, the saturation throughput is the same for all the N nodes and the AP. The difference between the analysis and simulation results occurs due to the decoupling approximations, but is small.

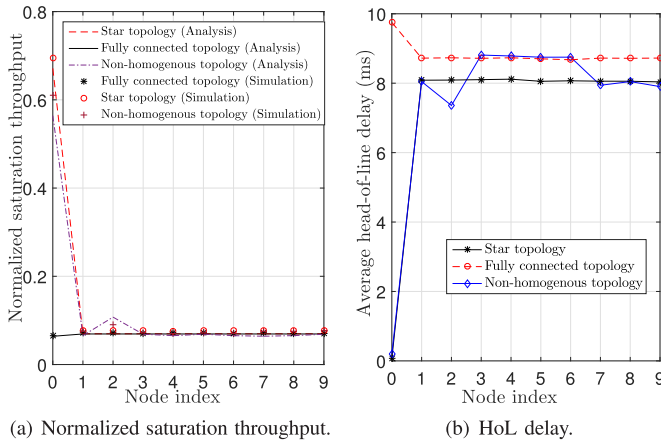


Fig. 3. Normalized saturation throughput and HoL delay of the AP and the N nodes for three specific network topologies.

Fig. 3(b) plots the HoL delay as a function of the node index. We see that the HoL delay of the AP is the lowest among all nodes in the non-homogeneous and star topologies. This is because it gets to transmit more often than the N nodes due to its FD capability. However, in the fully connected topology, it is marginally more than that of the N nodes. This is because, in the AP-cum-node-initiated scenario, when one node transmits an RTS packet along with the AP, the RTS packet transmitted by the node is successfully decoded at the AP while that of the AP collides. The HoL delay of node 2 is the lowest among the N nodes in the non-homogeneous topology, which is consistent with the results in Fig. 3(a).

B. Topology-Averaged Results

We now present results that are averaged over many network topologies, which are generated as follows. The interference link between two nodes is present with probability $1 - P_h$ and is absent with probability P_h ; we shall refer to P_h as the *hidden node probability*.

Fig. 4(a) compares the topology-averaged saturation throughput as a function of N for different values of P_h .⁴ We observe that not exploiting FD transmission opportunities in the AP-initiated scenario or using two-stage back-off to select transmitters leads to a lower throughput compared to AFD-MAC for $P_h > 0$. For example, when $N = 15$ and $P_h = 0.4$, not exploiting FD in the AP-initiated scenario and using a two-stage back-off timer reduces the throughput by 5.6% and 10.3%, respectively. Furthermore, the total uplink and downlink throughputs turn out to be comparable in AFD-MAC. For example, when $N = 15$, their ratio is 0.96 and 1.00 for $P_h = 0.2$ and 0.4, respectively (figure not shown). This is desirable in practice because the downlink traffic is typically more than the uplink traffic.

Fig. 4(b) plots the topology-averaged HoL delay of the AP and the N nodes as a function of N for different values of P_h . To avoid clutter, only AFD-MAC and 802.11 HD MAC are compared. The presence of hidden nodes affects the HoL

⁴The saturation throughputs of 802.11 HD MAC for $P_h = 0.2$ and 0.4 are marginally lower than for $P_h = 0$. They are not shown in the figure in order to avoid clutter.

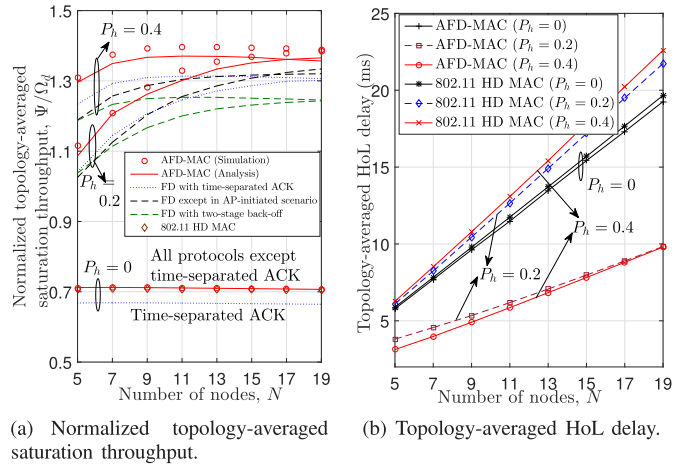


Fig. 4. Zoomed-in comparison of normalized topology-averaged saturation throughput and topology-averaged HoL delay as a function of N .

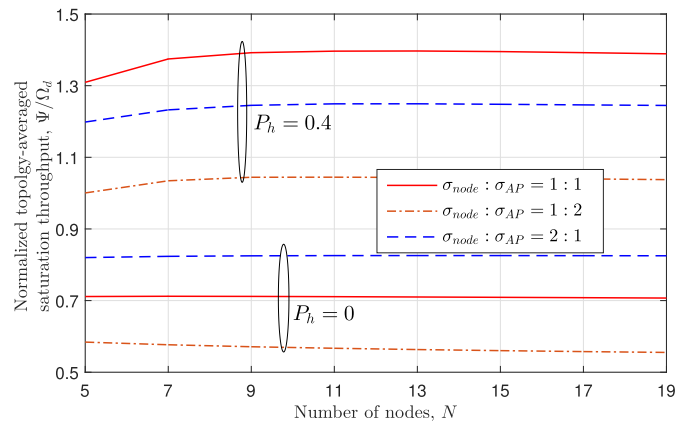


Fig. 5. Effect of asymmetry in the packet transmission durations: Zoomed-in comparison of normalized topology-averaged saturation throughput as a function of N for different ratios of the uplink and downlink data packet durations ($\sigma_{AP} = 692 \mu\text{s}$).

delays of the two protocols differently. For 802.11 HD MAC, it increases as P_h increases. On the other hand, it is much lower for AFD-MAC and decreases as P_h increases. Also, the HoL delay increases linearly with N in both protocols.

Fig. 5 studies the effect of asymmetry in the uplink and downlink packet durations. It plots the normalized saturation throughput, summed over the AP and the N nodes, as a function of N for three different ratios of the AP and node data packet durations. The saturation throughput is the largest when the packet durations are the same. This is because the AP can utilize its FD capability during the entire transmission. However, for $P_h = 0$, the saturation throughput is higher for $\sigma_{node}/\sigma_{AP} = 2$. This is because the N nodes, which have larger data packets than the AP, together transmit more frequently than the AP.

C. Impact of Imperfect SIC

Fig. 6 plots the normalized topology-averaged saturation throughput as a function of N . It is generated using the following parameters: $P_{TX} = 15$ dBm, $T = 298$ K, $B = 20$ MHz, and $F = 10$ dB. To compute P_{RX} , the path-loss

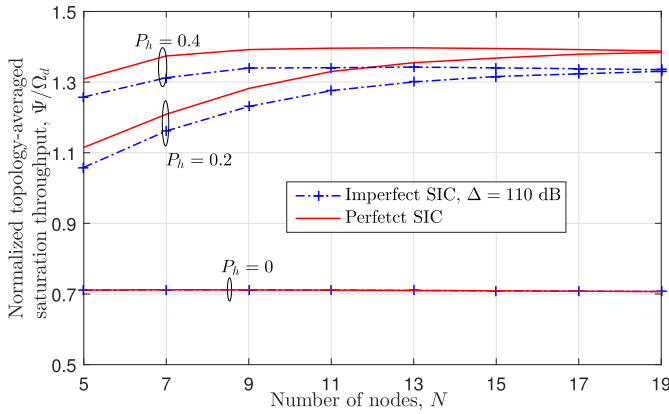


Fig. 6. Effect of imperfect SIC: Zoomed-in comparison of normalized topology-averaged saturation throughput as a function of N for different hidden node probabilities.

parameters, which are based on the model in [34, Chap. 2.6], are: carrier frequency $f_c = 5$ GHz, path-loss exponent $\eta = 3.8$, distance $d = 50$ m, and critical distance $d_0 = 10$ m. Also, we use the PER curves in [29, Fig. 4] to compute the PER values.

For $P_h = 0$, since there are no hidden nodes, the AP always transmits in HD. Therefore, imperfect SIC has no impact. On the other hand, for $P_h = 0.2$ and 0.4 , the saturation throughput decreases because of imperfect SIC. For example, it decreases by 4.5% for $N = 7$ and 9.3% for $N = 17$ when $P_h = 0.4$. This is because the SINR decreases from 12.9 dB with perfect SIC to 11.4 dB when $\Delta = 110$ dB. The PER at this SINR is 7.8%. We observe a similar change for $P_h = 0.2$ as well.

V. CONCLUSION AND FUTURE WORK

We proposed the AFD-MAC protocol that leveraged the distributed timer back-off and the RTS-CTS mechanism of the widely-used 802.11 HD MAC protocol for the asymmetric network model in which each node could have a different number and set of hidden nodes. The renewal-theoretic fixed-point analysis of the protocol, which was based on the collision model, led to an accurate characterization of the saturation throughput in the presence of hidden nodes. We saw that AFD-MAC increased the saturation throughput by a factor as large as two and it reduced the HoL delay by more than half compared to the conventional 802.11 HD MAC. The extent of the improvement depended on the network topology, asymmetry in the uplink and downlink data packet durations, and extent of SIC at the AP. An interesting avenue for future work is to investigate alternate, more physically realistic abstractions such as the capture model.

APPENDIX

A. Brief Proof of Claim 1

1) *Evaluation of s_i* : Node i is a secondary transmitter when the AP transmits an RTS packet successfully to a destination node $l \neq i$ in the AP-initiated scenario, and it then selects node i to transmit in the uplink. This occurs with probability

$(\beta_0/N) \left[\prod_{k=1}^N (1 - \beta_k) \right] 1_{\{i \in \mathcal{N}_l^c\}} / |\mathcal{N}_l^c|$. Summing this probability over all $l \neq i$ yields (4).

2) *Evaluation $\mathbb{E} [R_i^{(j)}]$* : From the law of total expectation, we have

$$\mathbb{E} [R_i^{(j)}] = \sum_{k=1}^{L+1} k \mathbf{P} (R_i^{(j)} = k). \quad (18)$$

When $1 \leq k \leq L$, $R_i^{(j)}$ equals k if: (i) $(k - 1)$ previous RTS packet transmission attempts of node i for data packet j are unsuccessful and the k^{th} transmission attempt is successful, or (ii) all k attempts are unsuccessful and node i becomes a secondary transmitter before its $(k + 1)^{\text{th}}$ RTS packet transmission attempt. Therefore, for $1 \leq k \leq L$, we have

$$\begin{aligned} \mathbf{P} (R_i^{(j)} = k | w_0, w_1, \dots, w_k) \\ = \gamma_i^{k-1} \left[\prod_{m=0}^{k-1} (1 - s_i)^{w_m+1} \right] \\ \times \left[(1 - \gamma_i) + \gamma_i s_i \sum_{n=1}^{w_k+1} (1 - s_i)^{n-1} \right]. \end{aligned} \quad (19)$$

In the $(L + 1)^{\text{th}}$ transmission attempt, the data packet is either successfully transmitted or dropped. For this, node i must not be a secondary transmitter in any of the previous $\sum_{k=0}^L (w_k + 1)$ slots. Thus,

$$\mathbf{P} (R_i^{(j)} = L + 1 | w_0, w_1, \dots, w_L) = \gamma_i^L (1 - s_i)^{\sum_{k=0}^L (w_k+1)}. \quad (20)$$

Averaging the probabilities in (19) and (20) with respect to w_0, w_1, \dots, w_L and substituting in (18), we get

$$\begin{aligned} \mathbb{E} [R_i^{(j)}] = \sum_{k=1}^{L+1} k \gamma_i^{k-1} \left[\prod_{m=0}^{k-1} z_m(s_i) \right] \\ - \sum_{k=1}^L k \gamma_i^k \left[\prod_{m=0}^k z_m(s_i) \right], \end{aligned} \quad (21)$$

where $z_m(s_i)$ is defined in the claim statement.

3) *Evaluating $\mathbb{E} [\chi_i^{(j)}]$* : It is given by

$$\mathbb{E} [\chi_i^{(j)}] = \sum_{k=0}^L \bar{T}_k(s_i, \gamma_i) + \bar{T}_{\text{drp}}(s_i, \gamma_i), \quad (22)$$

where $\bar{T}_k(s_i, \gamma_i)$ and $\bar{T}_{\text{drp}}(s_i, \gamma_i)$ are defined in the claim statement.

a) *Evaluation of $\bar{T}_k(s_i, \gamma_i)$* : Let $T_{k,i}$ be the average duration of a renewal cycle in which a packet is successfully transmitted after k collisions given the back-off timer values w_0, w_1, \dots, w_k . Then,

$$T_{k,i} = \sum_{n=\sum_{l=0}^{k-1} (w_l+1)+1}^{\sum_{l=0}^k (w_l+1)} n \mathbf{P} (\chi_i^{(j)} = n | w_0, w_1, \dots, w_k). \quad (23)$$

When $\sum_{l=0}^{k-1} (w_l + 1) + 1 \leq n \leq \sum_{l=0}^k (w_l + 1) - 1$, we know that $\chi_i^{(j)} = n$ if: (i) node i has transmitted its RTS packet k

times, all of which have collided; and (ii) it is a secondary transmitter in slot n but not in the previous $(n - 1)$ slots. Therefore,

$$\mathbb{P}\left(\chi_i^{(j)} = n | w_0, w_1, \dots, w_k\right) = \gamma_i^k s_i (1 - s_i)^{n-1}. \quad (24)$$

When $\chi_i^{(j)} = \sum_{l=0}^k (w_l + 1)$, the back-off timer of the node expires. Therefore, this event occurs if node i is a secondary transmitter in slot n or it transmits its RTS packet successfully at the end of the slot. Hence,

$$\begin{aligned} \mathbb{P}\left(\chi_i^{(j)} = \sum_{l=0}^k (w_l + 1) | w_0, w_1, \dots, w_k\right) \\ = \gamma_i^k (1 - s_i)^{\sum_{l=0}^k (w_l + 1) - 1} [s_i + (1 - \gamma_i)(1 - s_i)]. \end{aligned} \quad (25)$$

Substituting (24) and (25) in (23), and simplifying further, we get

$$\begin{aligned} T_{k,i} &= \gamma_i^k s_i \sum_{l=0}^{k-1} \left[(w_l + 1) \prod_{m=0}^{k-1} (1 - s_i)^{w_m + 1} \right] \\ &\quad \times \sum_{n=1}^{w_k + 1} (1 - s_i)^{n-1} + \gamma_i^k s_i \left[\sum_{n=1}^{w_k + 1} n (1 - s_i)^{n-1} \right] \\ &\quad \times \left[\prod_{m=0}^{k-1} (1 - s_i)^{w_m + 1} \right] + (1 - \gamma_i) \gamma_i^k \\ &\quad \times \left[\prod_{m=0}^k (1 - s_i)^{w_m + 1} \right] \left[\sum_{l=0}^k (w_l + 1) \right]. \end{aligned} \quad (26)$$

Substituting the identities $\sum_{n=1}^{w_k + 1} (1 - s_i)^{n-1} = [1 - (1 - s_i)^{w_k + 1}] / s_i$ and $\sum_{n=1}^{w_k + 1} n (1 - s_i)^{n-1} = [(1 - (1 - s_i)^{w_k + 1}) - s_i (w_k + 1) (1 - s_i)^{w_k + 1}] / s_i^2$ in (26) and using $\bar{T}_k(s_i, \gamma_i) = \mathbb{E}[T_{k,i}]$ yields (6).

b) Evaluation of $\bar{T}_{\text{drp}}(s_i, \gamma_i)$: The data packet is dropped if the RTS packets collided in $(L + 1)$ transmission attempts and the node was not a secondary transmitter in any of the slots $1, \dots, \sum_{k=0}^L (w_k + 1)$. This occurs with probability $\eta_{\text{drp}}^{(i)} = \gamma_i^{L+1} \prod_{m=0}^L (1 - s_i)^{w_m + 1}$. For this case, $\chi_i^{(j)} = \sum_{k=0}^L (w_k + 1)$. Hence,

$$\begin{aligned} \bar{T}_{\text{drp}}(s_i, \gamma_i) &= \mathbb{E}\left[\gamma_i^{L+1} \left(\prod_{m=0}^L (1 - s_i)^{w_m + 1} \right) \right. \\ &\quad \left. \times \sum_{k=0}^L (w_k + 1) \right]. \end{aligned} \quad (27)$$

Simplifying (27) yields (7). Dividing (21) by (22) yields (3).

B. Brief Proof of Claim 2

1) Evaluation of s'_i : The AP transmits as a secondary transmitter to node i if a node $k \in \mathcal{N}_i^c$ transmits an RTS packet successfully to the AP and then the AP selects node i for its transmission. Node k transmits its RTS packet successfully if no node transmits an RTS packet in the slot in which it transmits and none of its hidden nodes transmit in the preceding or succeeding slots. The probability of this event is $(1 - \beta_0) \beta_k \left[\prod_{l=1, l \neq k}^N (1 - \beta_l) \right] \left[\prod_{l \in \mathcal{N}_k^c} (1 - \beta_l) \right] / |\mathcal{N}_k^c|$. Summing it over all $k \in \mathcal{N}_i^c$ yields (9).

2) Evaluation of $\mathbb{E}[R_0^{(j)}]$ and $\mathbb{E}[\chi_0^{(j)}]$: In a manner similar to Appendix A, the average number of transmission attempts when the AP transmits a data packet to a destination node $i \in \mathbb{N}$ is $\sum_{k=1}^{L+1} k \Gamma_i^{k-1} \left[\prod_{m=0}^{k-1} z_m(s'_i) \right] - \sum_{k=1}^L k \Gamma_i^k \left[\prod_{m=0}^k z_m(s'_i) \right]$. Since the AP transmits to node i with probability $1/N$, we get

$$\begin{aligned} \mathbb{E}\left[R_0^{(j)}\right] &= \frac{1}{N} \sum_{i=1}^N \left(\sum_{k=1}^{L+1} k \Gamma_i^{k-1} \left[\prod_{m=0}^{k-1} z_m(s'_i) \right] \right. \\ &\quad \left. - \sum_{k=1}^L k \Gamma_i^k \left[\prod_{m=0}^k z_m(s'_i) \right] \right). \end{aligned} \quad (28)$$

Similarly, the mean renewal interval duration $\mathbb{E}[\chi_0^{(j)}]$ of the AP is given by

$$\mathbb{E}\left[\chi_0^{(j)}\right] = \frac{1}{N} \sum_{i=1}^N \left(\sum_{k=0}^L \bar{T}_k(s'_i, \Gamma_i) + \bar{T}_{\text{drp}}(s'_i, \Gamma_i) \right). \quad (29)$$

Dividing (28) by (29) yields (8).

C. Proof of Claim 3

We evaluate the conditional collision probabilities of the N nodes and the AP separately.

1) Node i , for $i \in \mathbb{N}$: In the AP-cum-node-initiated scenario, an RTS packet transmitted by node i is successful if no other node transmits an RTS packet to the AP simultaneously. The probability of this event is $\beta_0 \prod_{j=1, j \neq i}^N (1 - \beta_j)$. In the node-initiated scenario, an RTS packet transmitted by node i is successful if none of its hidden nodes transmit in the preceding or succeeding slots. The probability of this event is $(1 - \beta_0) \left[\prod_{j=1, j \neq i}^N (1 - \beta_j) \right] \left[\prod_{j \in \mathcal{N}_i^c} (1 - \beta_j)^2 \right]$. Therefore,

$$\begin{aligned} \gamma_i &= 1 - (1 - \beta_0) \left[\prod_{j=1, j \neq i}^N (1 - \beta_j) \right] \left[\prod_{j \in \mathcal{N}_i^c} (1 - \beta_j)^2 \right] \\ &\quad - \beta_0 \left[\prod_{j=1, j \neq i}^N (1 - \beta_j) \right]. \end{aligned} \quad (30)$$

2) AP: An RTS packet transmitted by the AP to a destination node $i \in \mathbb{N}$ collides if any node in \mathcal{N}_i transmits an RTS packet simultaneously. Therefore,

$$\Gamma_i = 1 - \prod_{j \in \mathcal{N}_i} (1 - \beta_j). \quad (31)$$

D. Proof of Claim 4

We evaluate the average number of bits transmitted by the AP and the N nodes separately below.

1) Evaluation of $\mathbb{E}[\theta_i]$, for $i \in \mathbb{N}$: Let $\pi_p(i)$ and $\pi_s(i)$ be the probabilities of node i transmitting a data packet as a primary transmitter and secondary transmitter, respectively, in a renewal interval given that the channel is not idle. Hence,

$$\mathbb{E}[\theta_i] = \phi_i (\pi_p(i) + \pi_s(i)). \quad (32)$$

Evaluation of $\pi_p(i)$: Node i transmits as a primary transmitter in the following scenarios:

1) In the node-initiated scenario, it is a primary transmitter if it is the only node that transmits an RTS packet and all its hidden nodes are idle in the preceding and succeeding slots. This occurs with probability $P_1(i) = \frac{\beta_i(1-\beta_0)[\prod_{j=1, j \neq i}^N (1-\beta_j)][\prod_{j \in \mathcal{N}_i^c} (1-\beta_j)^2]}{1 - \prod_{k=0}^N (1-\beta_k)}$. The denominator term $1 - \prod_{k=0}^N (1-\beta_k)$ is because of our conditioning on the event that the channel is not idle.

2) In the AP-cum-node-initiated scenario, it is a primary transmitter only if it and the AP transmit their RTS packets in the same slot and the remaining nodes are idle. The probability $P_2(i)$ of this event is $\beta_0\beta_i \left[\prod_{j=1, j \neq i}^N (1-\beta_j) \right] / \left[1 - \prod_{k=0}^N (1-\beta_k) \right]$.

Since the above two events are mutually exclusive, we get $\pi_p(i) = P_1(i) + P_2(i)$. This yields

$$\pi_p(i) = \frac{1}{1 - \prod_{k=0}^N (1-\beta_k)} \left(\beta_0 \left[\prod_{j=1, j \neq i}^N (1-\beta_j) \right] + \beta_i(1-\beta_0) \prod_{j=1, j \neq i}^N (1-\beta_j) \left[\prod_{j \in \mathcal{N}_i^c} (1-\beta_j)^2 \right] \right). \quad (33)$$

Evaluation of $\pi_s(i)$: From the discussion in Appendix A, it can be seen that

$$\pi_s(i) = \frac{\beta_0 \prod_{k=1}^N (1-\beta_k)}{N \left[1 - \prod_{k=0}^N (1-\beta_k) \right]} \sum_{j=1, j \neq i}^N \frac{1_{\{i \in \mathcal{N}_j^c\}}}{|\mathcal{N}_j^c|}. \quad (34)$$

Substituting (33) and (34) in (32) and simplifying yields (13).

2) *Evaluation of $\mathbb{E}[\theta_0]$:* As above, let $\pi_p(0)$ and $\pi_s(0)$ be the probabilities of the AP transmitting a data packet as a primary transmitter and secondary transmitter, respectively, in a renewal interval given that the channel is not idle. We have

$$\mathbb{E}[\theta_0] = \phi_0 (\pi_p(0) + \pi_s(0)). \quad (35)$$

Evaluation of $\pi_p(0)$: The AP transmits data packets as a primary transmitter in the following scenarios depending on whether its RTS packet transmission is successful or not.

3) *RTS Packet is Successful:* The RTS packet transmitted by the AP to a destination node i is successful with probability $(\beta_0/N) \left[\prod_{j \in \mathcal{N}_i} (1-\beta_j) \right] / \left(\left[1 - \prod_{k=0}^N (1-\beta_k) \right] \right)$.

4) *RTS Packet Collides:* If the RTS packet transmitted by the AP to node i collides with that sent by node j , then the AP can still transmit a data packet to a hidden node of j if it successfully decodes node j 's RTS packet. Here, i and j can even be the same. This occurs with probability $\frac{\beta_0 \sum_{j \in \mathcal{N}_i} \beta_j \left[\prod_{k=1, k \neq j}^N (1-\beta_k) \right] 1_{\{|\mathcal{N}_j^c| \neq 0\}}}{N \left[1 - \prod_{k=0}^N (1-\beta_k) \right]}$.

Summing the above probabilities over all $i \in \mathbb{N}$, we get

$$\pi_p(0) = \frac{\beta_0}{N \left[1 - \prod_{k=0}^N (1-\beta_k) \right]} \sum_{i=1}^N \left(\prod_{j \in \mathcal{N}_i} (1-\beta_j) + \sum_{j \in \mathcal{N}_i} \beta_j \left[\prod_{k=1, k \neq j}^N (1-\beta_k) \right] 1_{\{|\mathcal{N}_j^c| \neq 0\}} \right). \quad (36)$$

Evaluation of $\pi_s(0)$: In the node-initiated scenario, if an RTS packet transmitted by a node i is successful, then the AP transmits a data packet in parallel to one of the hidden nodes of i as a secondary transmitter. From the above discussions, it can be seen that the probability of this event is $\frac{(1-\beta_0)\beta_i \left[\prod_{j=1, j \neq i}^N (1-\beta_j) \right] \left[\prod_{j \in \mathcal{N}_i^c} (1-\beta_j)^2 \right] 1_{\{|\mathcal{N}_i^c| \neq 0\}}}{1 - \prod_{k=0}^N (1-\beta_k)}$. Summing it over all $i \in \mathbb{N}$, we get

$$\pi_s(0) = \frac{1-\beta_0}{1 - \prod_{k=0}^N (1-\beta_k)} \sum_{i=1}^N \beta_i \left[\prod_{j=1, j \neq i}^N (1-\beta_j) \right] \times \left[\prod_{j \in \mathcal{N}_i^c} (1-\beta_j)^2 \right] 1_{\{|\mathcal{N}_i^c| \neq 0\}}. \quad (37)$$

Substituting (36) and (37) in (35) and simplifying yields (14).

E. Proof of Claim 5

1. *Evaluation of \bar{T}_{idle} :* The idle period duration exceeds λ slots if no node transmits an RTS packet in slots $1, \dots, \lambda$. Therefore, $P(T_{idle} > \lambda) = \left[\prod_{k=0}^N (1-\beta_k) \right]^\lambda$. Since T_{idle} is a positive integer-valued RV, its average is given by

$$\begin{aligned} \bar{T}_{idle} &= \sum_{\lambda=0}^{\infty} P(T_{idle} > \lambda) = \sum_{\lambda=0}^{\infty} \left[\prod_{k=0}^N (1-\beta_k) \right]^\lambda \\ &= \left[1 - \prod_{k=0}^N (1-\beta_k) \right]^{-1}. \end{aligned} \quad (38)$$

2. *Evaluation of \bar{T}_s :* We sum the contributions from the following scenarios, which track who transmits the RTS packet(s) at the end of the idle period.

1) *Node-Initiated Scenario:* In this scenario, as shown in Appendix D, a successful RTS packet transmission by a node i occurs with probability $P_1(i)$. If node i has hidden nodes, then the AP transmits a data packet to one of them utilizing its FD capability. Else, only node i transmits a data packet in the HD mode. Therefore, the duration of transmission $T_1(i)$ is $\max \left\{ T_{AP} 1_{\{|\mathcal{N}_i^c| \neq 0\}}, T_{node} \right\}$. Summing over all $i \in \mathbb{N}$, we get

$$\begin{aligned} \bar{T}_1 &= \sum_{i=1}^N P_1(i) T_1(i), \\ &= \frac{1-\beta_0}{1 - \prod_{k=0}^N (1-\beta_k)} \sum_{i=1}^N \max \left\{ T_{AP} 1_{\{|\mathcal{N}_i^c| \neq 0\}}, T_{node} \right\} \\ &\quad \times \beta_i \left[\prod_{j=1, j \neq i}^N (1-\beta_j) \right] \left[\prod_{j \in \mathcal{N}_i^c} (1-\beta_j)^2 \right]. \end{aligned} \quad (39)$$

2) *AP-Initiated Scenario*: In this scenario, all the N nodes are idle and the AP selects a destination node i uniformly from the set \mathbb{N} . Therefore, a successful RTS packet transmission to node i occurs with probability

$$P'_2 = \left(\frac{\beta_0}{N} \right) \frac{\prod_{j=1}^N (1 - \beta_j)}{1 - \prod_{k=0}^N (1 - \beta_k)}.$$

If node i has no hidden nodes, then only the AP transmits a data packet. Else, both AP and node i transmit data packets simultaneously. Therefore, the duration $T_2(i)$ of packet transmission is $\max \{T_{AP}, T_{\text{node}} \mathbf{1}_{\{|\mathcal{N}_i^c| \neq 0\}}\}$. Summing over all $i \in \mathbb{N}$, the contribution \bar{T}_2 is given by

$$\begin{aligned} \bar{T}_2 &= \sum_{i=1}^N P'_2 T_2(i) = \frac{\beta_0 \prod_{j=1}^N (1 - \beta_j)}{N \left[1 - \prod_{k=0}^N (1 - \beta_k) \right]} \\ &\quad \times \sum_{i=1}^N \max \left\{ T_{AP}, T_{\text{node}} \mathbf{1}_{\{|\mathcal{N}_i^c| \neq 0\}} \right\}. \end{aligned} \quad (41)$$

3) *AP-cum-Node-Initiated Scenario*: Consider first the case in which the AP transmits an RTS packet to a destination node i and a node, say j , simultaneously transmits an RTS packet to the AP. Here, i and j can be the same. The probability $P_3(i, j)$ of this event is

$$P_3(i, j) = \left(\frac{\beta_0 \beta_j}{N} \right) \frac{\prod_{k=1, k \neq j}^N (1 - \beta_k)}{1 - \prod_{k=0}^N (1 - \beta_k)}.$$

If nodes i and j are hidden from each other, then both AP and node j successfully transmit data packets to their respective destinations. The duration of transmission in this case is $\max \{T_{AP} \mathbf{1}_{\{|\mathcal{N}_j^c| \neq 0\}}, T_{\text{node}}\}$. When nodes i and j are not hidden from each other or they are the same, node i cannot decode the RTS packet from the AP due to the collision. In this case, the AP selects another destination node hidden from node j . Here, the transmission duration is $\max \{T_{AP}, T_{\text{node}}\}$. If node j has no hidden node, then only it transmits to the AP for a duration T_{AP} . Therefore, the transmission duration when nodes i and j are not hidden from each other is $\max \{T_{AP} \mathbf{1}_{\{|\mathcal{N}_j^c| \neq 0\}}, T_{\text{node}}\}$. Summing over all $i, j \in \mathbb{N}$, the contribution \bar{T}_3 from this case is

$$\begin{aligned} \bar{T}_3 &= \sum_{i=1}^N \sum_{j=1}^N P_3(i, j) T_3, \\ &= \frac{\beta_0}{\left[1 - \prod_{k=0}^N (1 - \beta_k) \right]} \sum_{i=1}^N \max \left\{ T_{AP} \mathbf{1}_{\{|\mathcal{N}_i^c| \neq 0\}}, T_{\text{node}} \right\} \\ &\quad \times \beta_i \left[\prod_{j=1, j \neq i}^N (1 - \beta_j) \right]. \end{aligned} \quad (42)$$

The other possibility is that multiple nodes simultaneously transmit RTS packets along with the AP. We ignore its contribution since its probability is negligible. Adding (40), (41), and (43) and simplifying further yields (16).

3. *Evaluation of $\bar{T}_{\text{no-tx}}$* : Conditioned on the channel not being idle, let η_1 denote the probability of no successful

data packet transmission in a renewal interval when the AP transmits an RTS packet that collides. Similarly, let η_2 be the corresponding probability when the AP is idle. Then,

$$\bar{T}_{\text{no-tx}} = T_{\text{abrt}} (\eta_1 + \eta_2), \quad (44)$$

where T_{abrt} is defined in the claim statement.

Evaluation of η_1 : No successful data packet transmission occurs if the RTS packet transmitted by the AP to its destination node i collides and the RTS packets transmitted by at least two nodes to the AP also collide. The probability of this event can be shown to be $\frac{\beta_0 \left(1 - \prod_{j \in \mathcal{N}_i^c} (1 - \beta_j) - \sum_{j \in \mathcal{N}_i^c} \beta_j \left[\prod_{k=1, k \neq j}^N (1 - \beta_k) \right] \right)}{N \left[1 - \prod_{k=0}^N (1 - \beta_k) \right]}$. Summing this over all $i \in \mathbb{N}$, we get

$$\begin{aligned} \eta_1 &= \frac{\beta_0}{N \left[1 - \prod_{k=0}^N (1 - \beta_k) \right]} \sum_{i=1}^N \left(1 - \prod_{j \in \mathcal{N}_i} (1 - \beta_j) \right. \\ &\quad \left. - \sum_{j \in \mathcal{N}_i^c} \beta_j \left[\prod_{k=1, k \neq j}^N (1 - \beta_k) \right] \right). \end{aligned} \quad (45)$$

Evaluation of η_2 : In the node-initiated scenario, an RTS packet transmitted by a node collides if multiple nodes transmit RTS packets in the same slot or its hidden nodes transmit in the preceding or succeeding slots. The probability of this event is $1 - \prod_{i=1}^N (1 - \beta_i) - \sum_{i=1}^N \beta_i \left[\prod_{j=1, j \neq i}^N (1 - \beta_j) \right] \left[\prod_{j \in \mathcal{N}_i^c} (1 - \beta_j) \right]^2$. Therefore,

$$\begin{aligned} \eta_2 &= \frac{(1 - \beta_0)}{1 - \prod_{k=0}^N (1 - \beta_k)} \left(1 - \prod_{i=1}^N (1 - \beta_i) \right. \\ &\quad \left. - \sum_{i=1}^N \beta_i \left[\prod_{j=1, j \neq i}^N (1 - \beta_j) \right] \left[\prod_{j \in \mathcal{N}_i^c} (1 - \beta_j) \right]^2 \right). \end{aligned} \quad (46)$$

Substituting (45) and (46) in (44) and simplifying further yields (17).

REFERENCES

- [1] A. Sabharwal, P. Schniter, D. Guo, D. W. Bliss, S. Rangarajan, and R. Wichman, "In-band full-duplex wireless: Challenges and opportunities," *IEEE J. Sel. Areas Commun.*, vol. 32, no. 9, pp. 1637–1652, Sep. 2014.
- [2] D. Bharadia, E. McMillin, and S. Katti, "Full duplex radios," in *Proc. ACM SIGCOMM*, Aug. 2013, pp. 375–386.
- [3] M. Jain *et al.*, "Practical, real-time, full duplex wireless," in *Proc. ACM MobiCom*, Sep. 2011, pp. 301–312.
- [4] A. Tang and X. Wang, "Balanced RF-circuit based self-interference cancellation for full duplex communications," *Ad Hoc Netw.*, vol. 24, pp. 214–227, Jan. 2015.
- [5] K. Sanada and K. Mori, "Throughput analysis for full duplex wireless local area networks with hidden nodes," in *Proc. IEEE CCNC*, Jan. 2019, pp. 1–4.
- [6] M. Duarte *et al.*, "Design and characterization of a full-duplex multi-antenna system for WiFi networks," *IEEE Trans. Veh. Technol.*, vol. 63, no. 3, pp. 1160–1177, Mar. 2014.
- [7] S. Goyal, P. Lui, O. Gurbuz, E. Erkip, and S. Panwar, "A distributed MAC protocol for full duplex radio," in *Proc. IEEE Asilomar Conf. Signals, Syst., Comput.*, Nov. 2013, pp. 788–792.
- [8] X. Wang, A. Tang, and P. Huang, "Full duplex random access for multi-user OFDMA communication systems," *Ad Hoc Netw.*, vol. 24, pp. 200–213, Jan. 2015.

- [9] M. Murad and A. M. Eltawil, "A simple full-duplex MAC protocol exploiting asymmetric traffic loads in WiFi systems," in *Proc. IEEE WCNC*, Mar. 2017, pp. 1–6.
- [10] Y. Liao, K. Bian, L. Song, and Z. Han, "Full-duplex MAC protocol design and analysis," *IEEE Commun. Lett.*, vol. 19, no. 7, pp. 1185–1188, Jul. 2015.
- [11] L. Song, Y. Liao, K. Bian, L. Song, and Z. Han, "Cross-layer protocol design for CSMA/CD in full-duplex WiFi networks," *IEEE Commun. Lett.*, vol. 20, no. 4, pp. 792–795, Apr. 2016.
- [12] W. Choi, H. Lim, and A. Sabharwal, "Power-controlled medium access control protocol for full-duplex WiFi networks," *IEEE Trans. Wireless Commun.*, vol. 14, no. 7, pp. 3601–3613, Jul. 2015.
- [13] J. Hu, B. Di, Y. Liao, K. Bian, and L. Song, "Hybrid MAC protocol design and optimization for full duplex Wi-Fi networks," *IEEE Trans. Wireless Commun.*, vol. 17, no. 6, pp. 3615–3630, Jun. 2018.
- [14] S. Kim, M. S. Sim, C.-B. Chae, and S. Choi, "Asymmetric simultaneous transmit and receive in WiFi networks," *IEEE Access*, vol. 5, no. 7, pp. 14079–14094, Jul. 2017.
- [15] C. Kai, T. Huang, L. Wang, and Y. Gu, "CSMA-based utility-optimal scheduling in the WLAN with a full-duplex access point," *IEEE Access*, vol. 6, pp. 41399–41409, Jul. 2018.
- [16] A. Tang and X. Wang, "A-Duplex: Medium access control for efficient coexistence between full-duplex and half-duplex communications," *IEEE Trans. Wireless Commun.*, vol. 14, no. 10, pp. 5871–5885, Oct. 2015.
- [17] K.-C. Hsu, K. C.-J. Lin, and H.-Y. Wei, "Inter-client interference cancellation for full-duplex networks," in *Proc. IEEE INFOCOM*, May 2017, pp. 1–9.
- [18] S.-Y. Chen, T.-F. Huang, K. C.-J. Lin, Y.-W. P. Hong, and A. Sabharwal, "Probabilistic-based adaptive full-duplex and half-duplex medium access control," in *Proc. IEEE GLOBECOM*, Dec. 2015, pp. 1–6.
- [19] N. Singh, D. Gunawardena, A. Proutiere, B. Radunovi, H. V. Balan, and P. Key, "Efficient and fair MAC for wireless networks with self-interference cancellation," in *Proc. IEEE WiOpt*, May 2011, pp. 94–101.
- [20] J. Y. Kim, O. Mashayekhi, H. Qu, M. Kazandjieva, and P. Levis, "Janus: A novel MAC protocol for full duplex radio," Dept. Comput. Sci., Stanford Univ., Stanford, CA, USA, Tech. Rep., 2013.
- [21] D. Marlahi and Ö. Gürbüz, "S-CW FD: A MAC protocol for full-duplex in wireless local area networks," in *Proc. IEEE WCNC*, Apr. 2016, pp. 1–6.
- [22] W. Cheng, X. Zhang, and H. Zhang, "Full-duplex spectrum-sensing and MAC-protocol for multichannel nontime-slotted cognitive radio networks," *IEEE J. Sel. Areas Commun.*, vol. 33, no. 5, pp. 820–831, May 2015.
- [23] C. Kim and C. Kim, "A full duplex MAC protocol for efficient asymmetric transmission in WLAN," in *Proc. ICNC*, Feb. 2016, pp. 1–5.
- [24] V. Ramaiyan, A. Kumar, and E. Altman, "Fixed point analysis of single cell IEEE 802.11e WLANs: Uniqueness and multistability," *IEEE/ACM Trans. Netw.*, vol. 16, no. 5, pp. 1080–1093, Oct. 2008.
- [25] A. Kumar, E. Altman, D. Miorandi, and M. Goyal, "New insights from a fixed point analysis of single cell IEEE 802.11 WLANs," in *Proc. INFOCOM*, Mar. 2005, pp. 1550–1561.
- [26] T. Issariyakul, D. Niyato, E. Hossain, and A. S. Alfa, "Exact distribution of access delay in IEEE 802.11 DCF MAC," in *Proc. IEEE Globecom*, Nov./Dec. 2005, pp. 2534–2538.
- [27] C. Chen, S. Hou, and S. Wu, "Saturation throughput analysis of an asymmetric full-duplex MAC protocol in WLANs with hidden terminals," *IEEE Access*, vol. 6, pp. 69948–69960, Nov. 2018.
- [28] G. Bianchi, "Performance analysis of the IEEE 802.11 distributed coordination function," *IEEE J. Sel. Areas Commun.*, vol. 18, no. 3, pp. 535–547, Mar. 2000.
- [29] H. Shafiee and M. Khoshgard, "Packet error rate and throughput estimation for link adaptation in wireless local area networks," in *Proc. IEEE ICCS*, Nov. 2002, pp. 852–856.
- [30] Z. Tong and M. Haenggi, "Throughput analysis for wireless networks with full-duplex radios," in *Proc. IEEE WCNC*, Mar. 2015, pp. 717–722.
- [31] R. Gallager, *Stochastic Processes*, 1st ed. Cambridge, U.K.: Cambridge Univ. Press, 2013.
- [32] A. Kumar, D. Manjunath, and J. Kuri, *Communication Networking: An Analytical Approach*, 1st ed. San Mateo, CA, USA: Morgan Kaufmann, 2004.
- [33] *IEEE Standard for Telecommunications and Information Exchange Between Systems—LAN/MAN Specific Requirements—Part 11: Wireless Medium Access Control (MAC) and physical layer (PHY) specifications: High Speed Physical Layer in the 5 GHz Band*, IEEE Standard 802.11a-1999, Dec. 1999, pp. 1–102.
- [34] A. Goldsmith, *Wireless Communications*, 1st ed. Cambridge, U.K.: Cambridge Univ. Press, 2005.



Rama Kiran received the B.E. degree in telecommunication engineering from the PES Institute of Technology, Bengaluru, India, in 2011, and the M.Tech. degree in electrical engineering from the Indian Institute of Technology (IIT), Kanpur, in 2014. He is currently pursuing the Ph.D. degree with the Department of Electrical Communication Engineering, Indian Institute of Science (IISc), Bengaluru. From 2014 to 2015, he was with NI Systems (India) Pvt., Ltd., Bengaluru, where he worked on the development and implementation of algorithms for LTE and IEEE 802.11b/af/ah wireless standards. His research interests include wireless communication, full-duplex communication, and next generation wireless standards.



Neelesh B. Mehta (S'98–M'01–SM'06–F'19) received the B.Tech. degree in electronics and communications engineering from IIT Madras in 1996, and the M.S. and Ph.D. degrees in electrical engineering from the California Institute of Technology, Pasadena, CA, USA, in 1997 and 2001, respectively. He is currently a Professor with the Department of Electrical Communication Engineering, Indian Institute of Science, Bengaluru. He is a fellow of the Indian National Science Academy (INSA), the Indian National Academy of Engineering (INAE), and the National Academy of Sciences India (NASI). He was a recipient of the Shanti Swarup Bhatnagar Award 2017 and the Swarnjayanti Fellowship. He has served on the Board of Governors for IEEE ComSoc from 2012 to 2015. He has served on the Executive Editorial Committee for IEEE TRANSACTIONS ON WIRELESS COMMUNICATIONS from 2014 to 2017, and as its Chair from 2017 to 2018.



Jestin Thomas received the B.Tech. degree in electronics and communication engineering from the National Institute of Technology (NIT), Calicut, in 2013, and the M.E. degree in telecommunication from the Indian Institute of Science (IISc), Bengaluru, in 2016. Since 2016, he has been with Maxlinear Inc. His research interests include full-duplex communication and signal processing algorithms for base station transceivers.